

Double proximity effect in hybrid planar superconductor-(normal metal/ferromagnet)-superconductor structures

T. E. Golikova,^{1,*} F. Hübner,² D. Beckmann,² I. E. Batov,¹ T. Yu. Karminskaya,³ M. Yu. Kupriyanov,³ A. A. Golubov,⁴ and V. V. Ryazanov^{1,5}

¹*Institute of Solid State Physics, RAS, 142432 Chernogolovka, Moscow District, Russia*

²*Institute of Nanotechnology, Karlsruhe Institute of Technology, 76021 Karlsruhe, Germany*

³*Lomonosov Moscow State University, Skobeltsyn Institute of Nuclear Physics, Moscow 119991, Russia*

⁴*Faculty of Science and Technology and MESA + Institute of Nanotechnology, University of Twente, 7500 AE Enschede, The Netherlands*

⁵*Russian Quantum Center, 2-d Spassalivkovsky pereulok 4, Moscow 119991, Russia*

(Received 24 February 2012; published 13 August 2012)

We have investigated the differential resistance of hybrid planar Al-(Cu/Fe)-Al submicron bridges at low temperatures and in weak magnetic fields. The structure consists of a Cu/Fe bilayer forming a bridge between two superconducting Al electrodes. In the superconducting state of Al electrodes, we have observed a double-peak peculiarity in differential resistance of the S-(N/F)-S structures at a bias voltage corresponding to the minigap. We claim that this effect (the splitting of the minigap) is due to an electron spin polarization in the normal metal which is induced by the ferromagnet. We have demonstrated that the double-peak peculiarity is converted to a single peak at a coercive applied field corresponding to zero magnetization of the Fe layer.

DOI: [10.1103/PhysRevB.86.064416](https://doi.org/10.1103/PhysRevB.86.064416)

PACS number(s): 74.45.+c, 74.78.Fk, 75.76.+j

I. INTRODUCTION

In superconductor–normal metal (SN) bilayers the superconducting proximity effect is responsible for the modification of the electron density of states (DOS) and the appearance of a minigap ε_g in the normal metal.¹ Thereby a normal-metal region close to the SN interface behaves as a genuine superconductor; i.e., there is an energy range ($-\varepsilon_g$, $+\varepsilon_g$) around the Fermi energy in which there are no available states for normal quasiparticles. This theoretical statement¹ was proved reliably in recent measurements of the local DOS.^{2–4} A minigap peculiarity becomes apparent in the differential conductance (resistance) spectra of SNS junctions side by side with the superconducting gap peculiarity of superconducting electrodes.^{5,6} In the case of a superconductor-ferromagnet (SF) bilayer the ferromagnetic exchange splitting of the spin subbands results in an energy shift of the corresponding minigap, which is asymmetric for the majority and the minority spin subbands;⁷ i.e., one can distinguish two minigap peculiarities in SF-DOS spectra. However, even in the case of diluted ferromagnets the exchange field E_{ex} is very large, so it is difficult to observe the minigap splitting on well-known proximity SF systems such as Nb-CuNi⁸ and Nb-PdNi.⁹ In Ref. 10, Yip first proposed to modify the DOS in the SN-proximity system by applying a magnetic “Zeeman” field h . Unfortunately, it is difficult to use applied magnetic fields in real SN experiments due to the “orbital” suppression of the superconducting electrodes. Recently, the authors of Ref. 11 have proposed to induce a weak “exchange field” h_{ef} via diffusion of spin-polarized electrons from F to N metal in NF bilayers, i.e., by using a complex NF bilayer as the weak link in a S-(N/F)-S structure. In this case an “effective” exchange field h_{ef} which is induced in the N layer is much smaller than the intrinsic exchange field E_{ex} of the neighboring F layer.

In this work, we report on an experimental observation of the “minigap splitting” in the SNF banks of S-(N/F)-S submicron-size bridges schematically shown in Fig. 1(b). The minigap splitting has been observed as a double-peak

peculiarity in the differential resistance of planar Al-(Cu/Fe)-Al junctions.

II. EXPERIMENT

Figure 1(a) shows a scanning electron microscopy (SEM) image of one of our samples together with the measurement scheme. The submicron-scale planar junctions were fabricated by means of the electron beam lithography and *in situ* shadow evaporation. First, a thin (10–15 nm) iron layer is deposited onto the oxidized silicon substrate, followed by the deposition of a 60 nm thick copper layer, so that in combination the NF bilayer bridge [$0.2 \times (0.3\text{--}0.6) \mu\text{m}^2$] is formed. Subsequently, a thick aluminum layer of around 100 nm is evaporated at a second angle in order to form the superconducting leads. We fabricated samples with different separation length L between the superconducting electrodes, ranging from 30 nm to 300 nm. All transport measurements were performed using the standard four-terminal method. As the specific resistance of the copper film ($\rho_N = 4.5 \mu\Omega \times \text{cm}$) is much smaller than the one of the iron film ($\rho_F = 70 \mu\Omega \times \text{cm}$), the main part of the current flows through the copper layer. The measurements at temperatures down to 0.3 K were performed in a shielded cryostat equipped with a superconducting solenoid. Two stages of RC filters were incorporated into the measurement system to eliminate the electrical noise.

III. EXPERIMENTAL RESULTS

In order to check that the iron layer forms a single domain magnetized along the S-(N/F)-S junction, reference iron structures with the same geometry and sizes as the N/F bilayers, but only with the ferromagnetic layer, were fabricated and subsequently investigated by means of magnetic-force-microscopy imaging (MFM). Figure 2(a) shows a MFM image of the iron bar at zero magnetic field together with the topographical image (AFM). The picture of magnetic poles is similar to the MFM images of iron nanostrips published

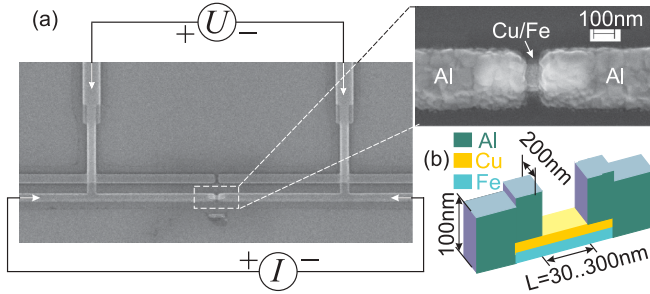


FIG. 1. (Color online) (a) SEM image of the Al-(Cu/Fe)-Al junction together with the measurement scheme. Inset shows the central part of the junction. (b) The schematic sketch of the sample with geometrical dimensions.

in Ref. 12. According to this work we dealt with practically uniform magnetized structure. The main magnetization is directed along the long axis of the rectangle but diverges from a dipolar configuration at the corners.¹³ Nonlocal spin-valve experiments on similar submicron iron structures indicate single-domain behavior, with coercive fields of about 200–500 Oe for magnetic fields applied along the element.¹⁴ To estimate the coercive field of the iron bar S-F-S (Al-Fe-Al) bridges with the same geometry but without the Cu layer were prepared. We have measured the magnetoresistance of the S-F-S bridge at $T = 4.2$ K using an in-plane magnetic field perpendicular to the Fe-bar easy axis [Fig. 2(b)]. The coercive field H_c (about 300 Oe) was determined from the maximum value of the resistance due to anisotropic magnetoresistance (AMR) effect (see, for example, Refs. 15 and 16). The observation of a finite coercive field suggests that the magnetization configuration deviates from the single-domain structure during magnetization reversal.

Resistive and Josephson characteristics of the planar junctions depend strongly on the spacing L between the aluminum electrodes as well as on the total length of Cu/Fe bilayers that were partly overlapped by the electrodes. The characteristics and their discussion will be given in detail in a later work.¹⁷ The Josephson supercurrent was observed in structures with L from 30 nm up to 130 nm. It is important to note that the

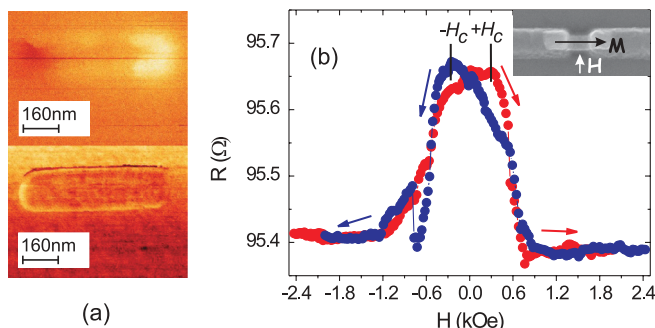


FIG. 2. (Color online) (a) The magnetic (top) and topographical (bottom) images of an iron bar with thickness of 10 nm. The images were edited by using WSxM (Ref. 18). (b) Resistance R of the Al-Fe-Al junction vs the external magnetic field H at the temperature 4.2 K. Inset: The SEM image of the sample with schematic view of direction of the external magnetic field H and magnetization M of the iron layer.

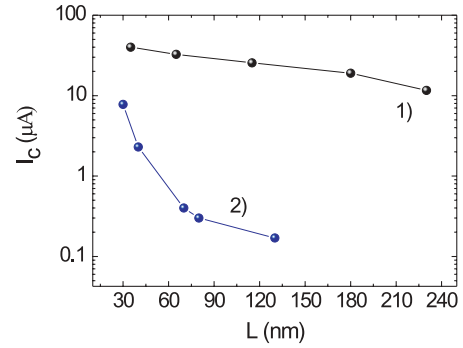


FIG. 3. (Color online) Dependencies of the critical current I_c on the sample length L for (1) Al-Cu-Al and (2) Al-(Cu/Fe)-Al nanobridges at $T = 0.4$ K.

coherent Josephson transport was suppressed significantly by addition of the extra ferromagnetic layer. Figure 3 presents the dependence of the critical current I_c vs L for the Al-(Cu/Fe)-Al junctions shown in Fig. 1 in comparison with the $I_c(L)$ dependence for control Al-Cu-Al structures fabricated by the same procedure but without the additional Fe layer. The critical currents of S-(N/F)-S junctions are much smaller than those for S-N-S junctions.

The weakening of the Josephson effect in S-(N/F)-S junctions with the addition of Fe can be naturally explained by effective spin polarization induced into the N layer. As a result, the effective coherence length in N becomes shorter and Josephson coupling is suppressed. The data of Ref. 19 indicate that the spin-diffusion length in Cu is as large as $1 \mu\text{m}$ at 1 K, which is larger than the bridge sizes.

To observe DOS peculiarities of the novel double-proximity structures we measured differential current-voltage characteristics by current-driven lock-in technique as well as the dc current-voltage characteristics of the structures. Figure 4(a) shows the differential resistance vs bias voltage for the Al-(Cu/Fe)-Al junction (S1) with the space $L = 130$ nm between superconducting electrodes at $T = 0.4$ K. The curve is symmetric with respect to the zero bias voltage; therefore only positive voltage values are shown. There are two types of peculiarities on the $dU/dI(U)$ dependence. The first one corresponds to the superconducting gap of aluminum $\Delta = 180 \mu\text{eV}$ and the second one is a double-peak peculiarity at the subgap energy $\varepsilon \approx 60 \mu\text{eV}$ which is much smaller than Δ .

IV. DISCUSSION

We suppose that the double-peak peculiarity in S-(N/F)-S transport is due to the presence of two spin-dependent minigaps in the normal-metal interlayer of SNF trilayered electrodes. The easiest way to check this idea with the spin-dependent minigap origin is to change the uniform state of the ferromagnet layer magnetization. The differential resistance of the S-(N/F)-S samples was measured in the presence of magnetic field H which increases from zero by small steps [see Fig. 4(b)]. Magnetic field was applied in plane of the sample perpendicular to the bridge, as it was for S-F-S structures shown in the Fig. 2(b) inset. One can see that at around 300 Oe the separation between the two peaks of the double-peak peculiarity decreases significantly

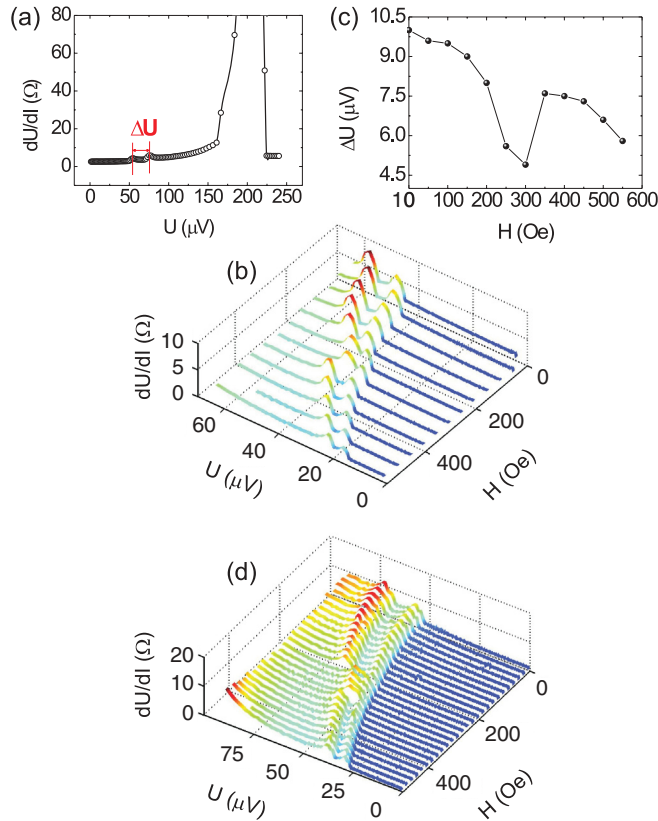


FIG. 4. (Color online) (a) Differential resistance dU/dI versus voltage U of Al-(Cu/Fe)-Al nanobridge S1 with length $L = 130$ nm at the temperature $T = 0.4$ K. The double peculiarity is signed with red lines; ΔU is the separation between peaks. (b) Differential resistance dU/dI versus voltage U and external magnetic field H of the sample S2. (c) The distance between two peaks on the dependence (b) versus external magnetic field H . (d) Differential resistance dU/dI versus voltage U and external magnetic field H of the sample S3. Double peak becomes single at the $H = H_c \approx 300$ Oe.

and then goes practically to the initial value at further increase of the magnetic field. The magnetic field of about 300 Oe coincides with the coercive field of the S-F-S reference structures. While the precise magnetization state at this field is unknown, a strongly inhomogeneous state can be expected, effectively reducing the induced exchange splitting in the N layer. The dependence of the double-peak splitting ΔU vs applied magnetic field H is shown in Fig. 4(c). Moreover it was observed for some samples that the double-peak peculiarity joined to single peak at about 300 Oe [Fig. 4(d)]. The position of the peculiarity is shifted to low voltages with increasing magnetic field because of the suppression of superconductivity in both the aluminum electrodes and the proximity region.

Below we briefly describe calculations of the minigap splitting in a SNF-NF structure with a trilayered electrode, i.e., the appearance of two minigaps for majority and minority spin systems in the N-layer due to the proximity effect from the superconductor and magnetic proximity effect due to a contact with a ferromagnet. For simplicity we shall discuss the case when F and N films are thin compared to the coherence lengths in these metals. Such simplification allows us to obtain a simple solution for the gap splitting but does not change

our conclusions qualitatively. We assume that the dirty limit conditions are fulfilled in the investigated structure; therefore one can use the quasiclassical Usadel equations for Green's functions which in θ parametrization have the form

$$\frac{\xi_{F,N}^2}{\tilde{\Omega}} \left\{ \frac{\partial^2}{\partial x^2} \theta_{F,N} + \frac{\partial^2}{\partial y^2} \theta_{F,N} \right\} - \sin \theta_{F,N} = 0. \quad (1)$$

Here $\tilde{\Omega} = \Omega + ih$, $h = E_{ex}/\pi T_C$, $\Omega = (2n+1)T/T_C$ are normalized Matsubara frequencies, E_{ex} is the exchange field which vanishes in N metal, and the $x(y)$ axes are parallel (perpendicular) to the FN interface with the origin at the boundary between the SNF trilayer and NF bilayer. Equations (1) should be supplemented by the boundary conditions (Ref. 20)

$$\gamma_{BN} \xi_N \frac{\partial}{\partial y} \theta_N = -\sin(\theta_S - \theta_N) \quad (2)$$

at the SN interface with $\gamma_{BN} = R_B/\rho_N \xi_N$ and

$$\xi_N \frac{\partial}{\partial y} \theta_N = \gamma \xi_F \frac{\partial}{\partial y} \theta_F, \quad \theta_N = \theta_F, \quad (3)$$

at the NF interface with $\gamma = \rho_N \xi_N / \rho_F \xi_F$ (we assumed that the FN interface is transparent). Here $\sin \theta_S = \Delta / \sqrt{\Omega^2 + \Delta^2}$ and Δ is the bulk pair potential of a superconductor. R_B is the specific resistance of the SN interface; $\rho_{S,F,N}$ and $\xi_{S,F,N}$ are the resistivities and the coherence lengths of the S, F, and N layers. We assume that $\gamma_{BN} \gg \max(1, \rho_S \xi_S / \rho_N \xi_N)$, so that suppression of superconductivity in the S electrode is negligibly small. At the free interfaces derivatives of θ functions are zero in the direction of the interface normal.

The problem (1)–(3) is reduced to one-dimensional equations for Green's functions in the NF bilayer under the S electrode θ_- (for $x < 0$) and Green's functions for the free FN bilayer θ_+ (for $x > 0$):

$$\eta^2 \frac{\partial^2}{\partial x^2} \theta_- - \sin(\theta_- - \theta_{-\infty}) = 0, \quad (4)$$

$$\mu^2 \frac{\partial^2}{\partial x^2} \theta_+ - \sin \theta_+ = 0,$$

where

$$\eta^2 = \frac{\gamma_{BM} (\gamma k \xi_F^2 + \xi_N^2) \cos \theta_{-\infty}}{\gamma_{BM} (\gamma k \tilde{\Omega} + \Omega) + \cos \theta_S}, \quad \mu^2 = \frac{\gamma k \xi_F^2 + \xi_N^2}{\gamma k \tilde{\Omega} + \Omega},$$

and $k = d_F \xi_N / (\xi_F d_N)$, $\gamma_{BM} = \gamma_{BN} d_N / \xi_N$. The solutions of the above equations are

$$\theta_+ = 4 \arctan \left[\tan \left(\frac{\theta_0}{4} \right) \exp \left(-\frac{x}{\mu} \right) \right],$$

$$\theta_- = \theta_{-\infty} + 4 \arctan \left[\tan \left(\frac{\theta_0 - \theta_{-\infty}}{4} \right) \exp \left(\frac{x}{\eta} \right) \right], \quad (5)$$

$$\theta_{-\infty} = \arctan \frac{\sin \theta_S}{\gamma_{BM} (\gamma k \tilde{\Omega} + \Omega) + \cos \theta_S},$$

$$\theta_0 = 2 \arctan \frac{\sin \frac{\theta_{-\infty}}{2}}{\cos \frac{\theta_{-\infty}}{2} + \eta/\mu},$$

and normalized DOS at energy ε is given by

$$\nu = \text{Re} [\cos \theta(-i\varepsilon + \delta)], \quad (6)$$

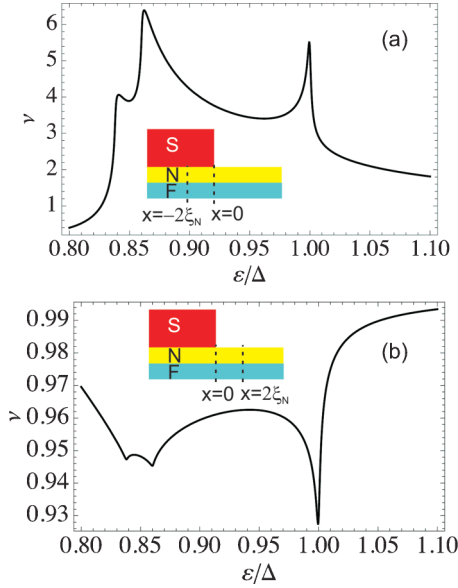


FIG. 5. (Color online) N-layer DOS of the SNF-NF structure versus normalized energy ε/Δ at $\gamma_{BM} = 0.3$, $h = 0.05$, $\gamma = 1$ for (a) $x = -2\xi_N$ and (b) $x = 2\xi_N$.

where $\delta = 10^{-3}$ was used in calculations.

Figure 5 shows the results of calculation of total DOS (summed over both spin subbands) from Eq. (6). It is seen that the peaks in DOS which for $x < 0$ occur at energies $\varepsilon = \Delta$, ε_+ , ε_- transform to dips for $x > 0$. The structure at energies ε_{\pm} corresponds to minigap splitting due to effective exchange field $h_{ef} = E_{ex}v_F d_F / (v_F d_F + v_N d_N)$, where $v_{N,F}, d_{N,F}$ are the normal-state densities of states and thicknesses of N and F layers. Interestingly, the double-peak structure at ε_{\pm} at $x < 0$ transforms to the double-dip structure in the bridge region ($x > 0$) at distances of the order of ξ_N . The energy separation ($\varepsilon_+ - \varepsilon_-$) between the peaks/dips can be estimated as $\varepsilon_+ - \varepsilon_- \simeq \gamma_{BM} h_{ef}$. For $E_{ex} = 0$, h_{ef} is also zero and these features merge into a single peak (dip).

The above results are obtained in the regime of the transparent NF interface ($\gamma_{BF} = 0$). For finite γ_{BF} , h_{ef} is renormalized by the factor $[1 + (\gamma_{BF} h d_F / \xi_F)^2]^{-1}$. This factor becomes small for large values of exchange field $h = E_{ex} / \pi T_c$ in the ferromagnet.

To interpret the observed double-peak structure in the resistance (dU/dI), we assume that the SN interface resistance is small compared to the resistance of the NF bridge connecting S electrodes; i.e., the electric field is distributed in the bridge area. In this case, the approach developed in Ref. 21 allows us to take into account nonequilibrium quasiparticle distribution in the NF bridge. In one-dimensional geometry and zero-temperature limit, the resistance is given by the expression

$$\frac{dU}{dI} = R_N \frac{1}{L} \int_0^L \frac{dx}{M(\varepsilon = eV, x)}, \quad (7)$$

where R_N is the normal-state resistance of the bridge and $M(x) = [\text{Re} \cos \theta(x)]^2 + [\text{Re} \sin \theta(x)]^2$ is the effective diffusion coefficient which has contributions from the normal DOS $\text{Re} \cos \theta$ and anomalous DOS $\text{Re} \sin \theta$. The latter has a behavior qualitatively similar to that of a normal DOS at subgap energies. Therefore, since $dU/dI \sim M^{-1}$, it is clear that the double-dip structure of the DOS in the bridge area shown in Fig. 5(b) should manifest itself as a double-peak structure in the resistance dU/dI vs U similar to that observed experimentally [see Fig. 4(a)]. Quantitative calculation of dU/dI is beyond the frame of our model due to the complex device geometry and a number of unknown parameters.

V. CONCLUSION

To conclude, we have observed experimentally a manifestation of the superconducting minigap splitting in the N layer in contact with both the superconductor and ferromagnet in the complex planar S-(N/F)-S system formed by the Al-(Cu/Fe)-Al submicron-size bridge. Such a splitting has to exist in SF bilayers also, but it is difficult to observe it there because of the large values of the exchange field for conventional ferromagnets. It has been demonstrated that the splitting occurs only for contacts to ferromagnetic layers with uniform magnetization and disappears when the applied magnetic field is close to the coercive field.

ACKNOWLEDGMENTS

We acknowledge A. V. Ustinov for support and useful discussions. The work was supported by grants from the Russian Academy of Sciences and the Russian Foundation for Basic Research.

*golt2@list.ru

¹A. A. Golubov and M. Yu. Kupriyanov, *J. Low Temp. Phys.* **70**, 83 (1988).

²S. Gueron, H. Pothier, N. O. Birge, D. Esteve, and M. H. Devoret, *Phys. Rev. Lett.* **77**, 3025 (1996).

³A. K. Gupta, L. Cretinon, N. Moussy, B. Pannetier, and H. Courtois, *Phys. Rev. B* **69**, 104514 (2004).

⁴H. le Sueur, P. Joyez, H. Pothier, C. Urbina, and D. Esteve, *Phys. Rev. Lett.* **100**, 197002 (2008).

⁵M. Meschke, J. T. Peltonen, J. P. Pekola, and F. Giazotto, *Phys. Rev. B* **84**, 214514 (2011).

⁶J. C. Cuevas, J. Hammer, J. Kopu, J. K. Viljas, and M. Eschrig, *Phys. Rev. B* **73**, 184505 (2006).

⁷A. A. Golubov, M. Yu. Kupriyanov, and Ya. V. Fominov, *Pis'ma Zh. Eksp. Teor. Fiz.* **75**, 223 (2002) [*JETP Lett.* **75**, 190 (2002)].

⁸V. A. Oboznov, V. V. Bol'ginov, A. K. Feofanov, V. V. Ryzanov, and A. I. Buzdin, *Phys. Rev. Lett.* **96**, 197003 (2006).

⁹T. Kontos, M. Aprili, J. Lesueur, and X. Grison, *Phys. Rev. Lett.* **86**, 304 (2001).

¹⁰S.-K. Yip, *Phys. Rev. B* **62**, R6127 (2000).

¹¹T. Yu. Karminskaya and M. Yu. Kupriyanov, *Pis'ma Zh. Eksp. Teor. Fiz.* **85**, 343 (2007) [*JETP Lett.* **85**, 286 (2007)].

- ¹²M. Hanson, O. Kazakova, P. Blomqvist, R. Wäppling, and B. Nilsson, *Phys. Rev. B* **66**, 144419 (2002).
- ¹³W. Rave and A. Hubert, *IEEE Trans. Magn.* **36**, 3886 (2000).
- ¹⁴D. Beckmann, H. B. Weber, and H. v. Löneysen, *Phys. Rev. Lett.* **93**, 197003 (2004).
- ¹⁵P. P. Freitas and T. S. Plaskett, *J. Appl. Phys.* **67**, 4901 (1990).
- ¹⁶R. McGuire and R. J. Potter, *IEEE Trans. Magn.* **11**, 1018 (1975).
- ¹⁷T. E. Golikova *et al.* (unpublished).
- ¹⁸I. Horcas, R. Fernandez, J. M. Gomez-Rodriguez, J. Colchero, J. Gomez-Herrero, and A. M. Baro, *Rev. Sci. Instrum.* **78**, 013705 (2007).
- ¹⁹T. Kimura, T. Sato, and Y. Otani, *Phys. Rev. Lett.* **100**, 066602 (2008).
- ²⁰M. Yu. Kuprianov and V. F. Lukichev, *Zh. Eksp. Teor. Fiz.* **94**, 139 (1988) [*Sov. Phys. JETP* **67**, 1163 (1988)].
- ²¹A. F. Volkov, A. V. Zaitsev, and T. M. Klapwijk, *Physica C* **210**, 21 (1993).